

1 Re-submitted to: *Environmental Pollution* (ENVPOL-D-14-00152)

2 Date: April 27, 2014

3

4 **Changes in the adsorption of bisphenol A, 17 α -ethinyl estradiol,**
5 **and phenanthrene on marine sediment in Hong Kong in relation**
6 **to the simulated sediment organic matter decomposition**

7 **Ying-heng Fei^{1,2}, Baoshan Xing³, Xiao-yan Li^{1*}**

8 ¹ Department of Civil Engineering, The University of Hong Kong, Hong Kong, China

9 ² Water Science Research Center, Guangzhou Institute of Advanced Technology, Chinese

10 Academy of Sciences, Guangzhou, China

11 ³ Department of Plant, Soil and Insect Sciences, University of Massachusetts, Amherst,

12 MA, USA

13 (*Corresponding author: phone: 852-28592659; fax: 852-28595337; e-mail: xlia@hkucc.hku.hk)

14

15 **Abstract**

16 Marine sediment with an input of particulate organic matter was incubated to simulate the
17 early aging process. On the sediment after various incubation periods, adsorption and
18 desorption tests were conducted for three selected organic micropollutants: bisphenol A
19 (BPA), 17 α -ethinyl estradiol (EE2), and phenanthrene (Phe). The results showed significant
20 sediment organic matter (SOM) decomposition during the incubation, and the SOM decay
21 and transformation had a profound impact on the adsorption of organic compounds by the
22 sediment. An increasing-delay-increasing pattern of change was observed for the SOM

23 normalized partition coefficients of EE2 and Phe. This change was accordant to the
24 transformation of SOM from labile organics into active biomass and its microbial products,
25 and finally into more condensed and humic-like substances. Comparison between the 3
26 model micropollutants indicates that the chemical adsorption behaviors were mostly affected
27 by their hydrophobic properties.

28 **Capsule:**

29 The early aging process of sediment organic matter led to an increasing-delay- increasing
30 pattern of change for the adsorption of hydrophobic organic pollutants by marine sediment.

31 **Key words:** adsorption; endocrine disrupting chemicals (EDCs); marine sediment; sediment
32 organic matter (SOM); SOM decomposition

33

34 **1 Introduction**

35 Sediment adsorption plays an important role in the fate of environmental pollutants in the
36 aquatic system. Sediment organic matter (SOM) has been shown to be the most important
37 component in the adsorption of hydrophobic organic pollutants (Chiou et al., 1979). The
38 adsorption of organic pollutants by SOM often has a stronger affinity compared to the
39 adsorption by mineral fractions, especially in SOM-rich soil or sediment (Cornelissen et al.,
40 2005; Voice and Weber, 1983; Zhao et al., 2010). A partition mechanism has been adopted
41 for nonionic organic adsorption by SOM (Chiou et al., 1979; Wang and Keller, 2009) in
42 which the partition coefficient, K_d , is used to quantify the adsorption capacity. The amount of
43 SOM in sediment has been shown to greatly influence the partition coefficients of
44 environmental contaminants on marine sediment (Gao et al., 1998; Xu et al., 2008).

45 Moreover, researchers have found that the adsorption of organic contaminants by
46 sediment is affected not only by the SOM content, but also by the chemical property of the
47 SOM (Cornelissen et al., 2005; Weber et al., 1999). Xing and Pignatello (1997) proposed that
48 various types of SOM in aged sediment could be compared to rubbery or/and glassy polymers
49 in explaining the sediment adsorption behaviors. Their dual model implying the impact of
50 SOM quality on the adsorption behaviors of sediment was supported by later studies (e.g.
51 Ran et al., 2007; Sun et al., 2010; Yang et al., 2010).

52 However, accounting for organic decomposition in sediment, the adsorption of pollutants
53 onto marine sediment with a rich organic input from particulate organic matter can be more
54 complicated. Under natural conditions, major fractions of labile SOM are biologically
55 mineralized within a few months, while more refractory fractions can be rather stable in
56 sediment (deBruyn and Gobas, 2004). Organic decomposition transforms SOM from less
57 stable organics into humic substances (Farnet et al., 2009; Plaza et al, 2009), which would
58 fundamentally affecting the adsorption behavior and capacity of the sediment (Fei et al., 2011;
59 Fei and Li, 2013). Prior studies have predicted the enrichment of chemicals in sediment
60 during SOM mineralization by theoretical analysis (Gobas and MacLean, 2003; Johnson et al.,
61 2001). However, few experimental studies have been conducted to prove the influence of
62 SOM degradation and transformation on the adsorption of environmental micropollutants by
63 the sediment. There is also a need to investigate the dynamic process of SOM decomposition
64 and its effect on sediment adsorption. Such an issue is of great importance for estuary or
65 marine areas such as Hong Kong and the Pearl River Delta in South China, where the
66 sediment receives a high SOM input, e.g. from stormwater runoff, sewage discharge and
67 mariculture activities (Wang et al., 2010). In our previous studies (Fei et al., 2011; Fei and Li,
68 2013), laboratory experiments were conducted to simulate the aging and decomposition of
69 SOM in artificial sediment, with flour powder as the fresh SOM input. With the SOM decay

70 during the sediment incubation, the adsorption of chemicals, including bisphenol A (BPA),
71 nonylphenol and tetracyclines, by the sediment was found to change significantly.

72 In the present study, the influence of SOM decomposition on the sediment adsorption
73 behavior was further investigated with following major modifications: (1) instead of artificial
74 sediment made of sand and clay, actual marine sediment was used for the experimental study;
75 (2) instead of flour powder (carbohydrate), fish food was selected as a better SOM to provide
76 a mixture of various particulate organic compounds; (3) three different chemicals were
77 selected as model micropollutants with different chemical structures and hydrophobic
78 properties. Based on the experimental results, sound theoretical analysis was conducted and
79 more comprehensive understanding was obtained. In addition, a conceptual model was
80 proposed to describe the dynamic change of chemical adsorption by the sediment in
81 connection to the SOM decomposition and transformation.

82

83 **2 Materials and Methods**

84 ***2.1 Sediment samples and sediment incubation***

85 Natural sediment was collected from depths 0 to 20 cm below the sediment surface at a
86 site (22°18.400/114°06.500) in Victoria Harbour, Hong Kong, and the sample was stored
87 under 4°C before use. After removing shells and gravels, the marine sediment was air-dried,
88 ground and homogenized, and dry sediment that passed through a 200 µm sieve was collected.
89 The organic content in the raw sediment was around 6.4%. Fish food was added as a fresh
90 SOM input into the sediment. Dried and ground fish food pellets (Hikari Lionhead, Japan)
91 were thoroughly mixed into the sediment at a dry weight ratio of 10%. The fish food as the
92 fresh SOM input was mostly insoluble, and its dry mass consisted of >61% of proteins, >8%
93 of lipids, <7% of fibers, <14% of other carbohydrates, and <10% of ashes, according to the
94 product information.

95 The sediment with a high SOM input was incubated in water to simulate the natural
96 decay and aging process. The sediment was placed into 30 separate glass dishes, each dish
97 being 6 cm in diameter and 1 cm in depth, and the sediment dishes were then placed on the
98 bottom of a large water tank. The tank was filled with 20 L of saline water made with reef
99 salt at a salinity of 10‰, which is close to the average salinity level in Deep Bay, Hong Kong,
100 where a large amount of SOM is received from Pearl River (Xu et al., 2010). The water in the
101 tank was circulated and aerated to ensure a dissolved oxygen (DO) level of 5 mg/L or higher
102 in the water over the sediment. The saline water was replaced weekly and the water
103 temperature varied between 22-24°C. Throughout the sediment incubation process, 4 dishes
104 of the incubated sediment were retrieved each time after different incubation periods (0, 15,
105 33, 54, 75, 96, and 125 d). The incubated sediment samples were then air-dried and ground
106 gently before SOM analysis and the subsequent adsorption tests.

107 **2.2 Sediment characterization**

108 The SOM content in a sediment sample was measured by means of LOI-550 (loss on
109 ignition at 550°C) (Beaudoin, 2003). As a simple and reliable measurement, the LOI results
110 have been to be consistent with the element-based organic carbon analysis (Fei et al., 2011).
111 In brief, the sediment sample was first dried in an oven at 105°C for 1 h. After cooling and
112 weighing, the dry solids was placed in a muffle oven and heated to 550°C for 15 min,
113 followed by cooling and weight measurement. The loss of weight after ignition was
114 determined as the amount of SOM in the sediment. The fraction of organic matter, f_{OM} , in the
115 raw or incubated sediment was calculated accordingly.

116 Humic substances were extracted from the sediment samples following the method
117 previously employed by Droussi et al. (2009). Briefly, humic matter was extracted by 0.1M
118 KOH for 7 times, the combined extract solution was precipitated by 6M H₂SO₄, and the
119 precipitate was then dissolved in 0.05M NaHCO₃ (pH=8.0) for analysis. Fluorescence

120 excitation and emission matrix (FEEM) was obtained by a fluorescence spectrophotometer
121 (F-7000, Hitachi, Japan) for the emission wavelength ranging 300-600 nm with the excitation
122 wavelength ranging 250-500 nm (Plaza et al., 2009). The absorbance at 465 nm (E_4) and 665
123 nm (E_6) of the humic solution was determined by a UV-VIS spectrophotometer (Lambda 12,
124 Perkin Elmer, USA), and the E_4/E_6 ratio was then calculated accordingly.

125 **2.3 Model micropollutants**

126 Endocrine disrupting chemicals (EDCs) have attracted public attention in recent years
127 due to the chronic harm they cause to the reproduction of organisms in the ecosystem (e.g.
128 Colborn et al., 1993; Collins, 2008). Two typical EDCs, BPA and 17 α -ethinyl estradiol (EE2)
129 were selected as the model chemicals for the sediment adsorption study. Another typical
130 non-polar organic contaminant, phenanthrene (Phe), which also has been indicated with
131 potential estrogenic activities in human colons (Van de Wiele et al., 2005), was selected as
132 well. Table 1 summarizes the chemical properties of the model compounds, including their
133 water solubility S_w and octanol-water partition coefficient K_{ow} values.

134 The chemicals were of analytical purity, with BPA (> 99%) purchased from Aldrich
135 (USA), EE2 (> 98%) from Sigma (USA), and Phe (> 98%) from Aldrich (USA). All of the
136 other chemicals and solvents used in the study were of analytical grade or better and were
137 obtained from Sigma-Aldrich (USA). BPA, EE2, and Phe were prepared in a background
138 solution consisting of 0.01 M CaCl_2 for a basic ionic strength and 200 mg/L of NaN_3 for the
139 inhibition of microbial activities during the adsorption tests (Xing and Pan, 2010). The
140 chemical solutions were prepared just before the adsorption experiment, and the solution pH
141 was 7.5.

142 **2.4 Adsorption experiments**

143 Adsorption tests were conducted to determine the isotherms of adsorption of the model
144 compounds on the sediment, using 11-mL or 40-mL screw-cap vials with Teflon-lined septa
145 (Xing and Pan, 2010; Xing and Pignatello, 1997). Briefly, a pre-determined amount of
146 sediment was placed in a series of vials, into which a model micropollutant solution of
147 different concentrations was subsequently added. The initial concentrations of BPA, EE2 and
148 Phe were in the ranges of 10-50 mg/L, 0.5-5 mg/L, and 0.1-0.5 mg/L, respectively. The vials,
149 which had nearly no headspace, were placed in a temperature-controlled shaking incubator
150 (Polyscience, USA) at 25°C and were rotated at the rate of 130 rpm. Upon completion of the
151 adsorption test, the sediment mixture from each vial was centrifuged at 4000 rpm for 5 min to
152 separate the liquid from the sediment, and the pollutant concentration in the aqueous phase
153 was measured using a high-performance liquid chromatography (HPLC).

154 The dry sediment/aqueous ratios were 0.7 g/10 mL, 0.3 g/10 mL, and 5 mg/40 mL for the
155 BPA, EE2, and Phe, respectively. The pH level of the solutions during the adsorption tests
156 was around 7.5. Our preliminary tests showed that the adsorption equilibrium could be
157 achieved in 24 hr for BPA or EE2 and in 72 hr for Phe. Losses of chemicals attributable to
158 glass wall adsorption or other causes were found to be less than 3%. Thus, the amount of the
159 chemical adsorbed by the sediment in each test vial could be determined by the difference
160 between the initial and final concentrations in the liquid phase.

161 After the adsorption experiment being completed, a desorption test was conducted on the
162 same sediment. For the desorption of BPA, the aqueous solution was replaced by 10 mL of
163 the clean background solution, and the sample vials were placed in the shaking incubator
164 (Polyscience, USA) at 25°C. After 48 hr, the sediment and solution were separated as
165 previously described, and the BPA concentration in the liquid phase was measured by the
166 HPLC. For EE2 desorption, due to the HPLC detection limit, only half (5 mL) of the liquid

167 was replaced with the clean solution, with the other half (5 mL) remaining in the vial. The
168 great hydrophobicity of Phe made its desorption into water extremely difficult. Sodium
169 dodecyl benzene sulfonate (SDBS), a surfactant often used in soil extraction (Zhao et al.,
170 2010), was therefore dosed (5 mL) into the sediment mixture at 10,000 mg/L for Phe
171 desorption.

172 **2.5 Chemical analysis**

173 The BPA, EE2, and Phe concentrations in water were measured by an HPLC (Waters
174 2695) with a C18 column (5 μ m, 2.1 \times 150 mm) for separation and a photodiode array detector
175 (Waters 2996) for quantification. For BPA and EE2, the mobile phase was a mixture of
176 Milli-Q water and acetonitrile (50:50, v/v). The flow rate was set at 0.5 mL/min, and the
177 sample injection volumes were 10 μ L for BPA and 50 μ L for EE2. Under this
178 chromatographic condition, the BPA peak appeared at around 6 min and the EE2 peak at
179 around 8 min. The area of the peak detected at a wavelength of 225 nm was used to quantify
180 the amount of the chemical detected (Mnif et al., 2012). The limits of detection and
181 quantification (LOD and LOQ) were 0.03 and 0.1 mg/L for BPA and 0.1 and 0.3 mg/L for
182 EE2. For Phe, the HPLC program was optimized by using acetonitrile as the mobile phase at
183 a flow rate of 0.5 mL/min. The Phe peak was obtained at around 7 min by detection at 250
184 nm (Zhao et al., 2010). Setting the injection volume at 10 μ L, the LOD and LOQ were 0.05
185 and 0.15 mg/L, respectively. The HPLC chromatographs for the chemical detections are
186 shown in the Supplementary Material (SI).

187 **2.6 Data analysis**

188 The results obtained in the sediment adsorption and desorption tests were used to
189 determine the adsorption and desorption isotherms. The isotherm data were arranged to fit the

190 following linear partition model (Eq. 1) and the Freundlich model (Eq. 2) (Voice and Weber,
191 1983):

$$192 \quad q_e = K_d C_e \quad (1)$$

$$193 \quad q_e = K_F C_e^{1/n} \quad (2)$$

194 where C_e and q_e are the equilibrium concentrations of the chemical in the aqueous phase and
195 sediment, respectively; K_d is the partition coefficient in the linear model; K_F and $1/n$ are the
196 affinity coefficient and curvature index, respectively, in the Freundlich equation. Microsoft
197 Excel 2010 was used for data analysis and curve fitting. Furthermore, K_d for partition is
198 normalized by the SOM content (f_{OM}) to obtain the organic matter normalized partition
199 coefficient K_{OM} (Eq. 3), i.e.

$$200 \quad K_{OM} = \frac{K_d}{f_{OM}} \quad (3)$$

201 Based on the comparison between the adsorption and desorption tests for a chemical by
202 the sediment, an hysteresis index (HI) can be calculated as follows (Wu and Sun, 2010),

$$203 \quad HI = \frac{K_{d(D)} - K_{d(A)}}{K_{d(A)}} \quad (4)$$

204 where $K_{d(D)}$ and $K_{d(A)}$ stand for the chemical partition coefficients obtained from the
205 desorption and adsorption tests, respectively. The HI value signifies the irreversibility of an
206 adsorption process, with $HI = 0$ representing completely reversible adsorption and a higher
207 HI value indicating more irreversible adsorption.

208

209 **3 Results and Discussion**

210 **3.1 SOM degradation and transformation**

211 The loaded SOM, fish food pallets, degradation was well observed during the sediment
212 incubation. The organic content in the sediment fell by 47% over 4 months (Fig. 1). The
213 SOM decomposition could be well fitted by multi-fractional first-order kinetic equations
214 (please refer to SI). SOM decay occurred more rapidly in the first month with a reduction of
215 around 40% of the initial f_{OM} . SOM reduction became much slower in the following 3 months.
216 Along with the SOM degradation, fresh SOM would be rapidly transformed into biomasses
217 and their metabolic products (Fei et al., 2011). Subsequent to SOM biodegradation, biomass
218 and microbial intermediate products would undergo further decay to form more condensed
219 geo-polymers such as fulvic acid, humic acid, and humin (Farnet et al., 2009; Plaza et al.,
220 2009).

221 Analysis on humic substances confirmed the humification-like process within the
222 sediment aging process. As shown in Fig 2., the FEEM features a primary peak at the
223 excitation/emission wavelength pair of 370/470 nm, and a secondary peak at around 450/540
224 nm. The E_4/E_6 ratio decreased significantly, as shown in Fig 3, indicating the accumulation of
225 aromatic contents and the condensation of the acidic humic substances in the sediment
226 samples (Droussi et al., 2009). Based on previous studies on organic incubation or
227 composting (e.g. Droussi et al., 2009; Guo et al., 2013), the elemental ratios of N/C, H/C, and
228 O/C would be increased during the organic matter decomposition process. The condensation
229 and humification process in sediment would change SOM into more humic-like matter
230 eventually with more carboxyl groups, alkyl carbon, and non-lignin aromatic structures
231 (Farnet et al., 2009).

232 **3.2 Adsorption and desorption of BPA**

233 Batch adsorption tests were conducted with the model chemical compounds to
234 characterize the change in the adsorption properties of the sediment after various periods of
235 incubation. The isotherms of BPA adsorption by the sediment fit well with either the linear
236 partition model or the Freundlich model ($R^2 \geq 0.98$) (Table 2 and Fig. 4). Chiou et al. (1979)
237 suggested that the adsorption of hydrophobic organic contaminants on soil or sediment could
238 be accurately described by the linear model with a partition coefficient indicating adsorption
239 capacity. Mathematically, the linear model can be considered a special case of the Freundlich
240 isotherm model when the curvature index $1/n$ in the Freundlich equation is close to 1 (Voice
241 and Weber, 1983). To allow simple and direct comparisons, the linear isotherm model and
242 related partition coefficients were used in most of the following analysis and discussion to
243 mathematically compare adsorption capacity between sediment samples after different
244 incubation periods.

245 For BPA, the partition coefficient K_d of the sediment cooperated with fish food pellets
246 increased by 8 times than the raw sediment (Table 2). The affinity coefficient in the
247 Freundlich model, K_F , showed more than 3 times of increase. It has been widely
248 demonstrated that a higher SOM content would lead to a higher adsorption affinity (e.g. Fei
249 et al., 2013; Sun et al., 2010; and Xu et al., 2008). Besides, the curvature index, $1/n$, also
250 increased from 0.71 to more than 0.97. For the raw sediment, the curved adsorption isotherm
251 has been commonly reported by others (e.g. Cornelissen et al., 2005; Gao et al., 1998; Voice
252 and Weber, 1983; etc.), and the linearity of the sorption isotherm is usually negatively related
253 with the SOM maturity (Cornelissen and Gustafsson, 2004).

254 For the SOM loaded and incubated sediment, K_d decreased by 69% from 35 to about 11
255 L/kg after 4 months of incubation. Most of the K_d decrease occurred in the first month,
256 accounting for a 54% decrease from the initial value. K_d fell by another 15% in the following

257 3 months. It is apparent that the loaded SOM influenced the adsorption capacity, and the
258 degradation of fresh SOM was the main cause of K_d reduction, as the K_d decreases observed
259 correlated well with f_{OM} reduction during the sediment incubation process. This is accordant
260 to our previous findings (Fei et al., 2011; Fei and Li, 2013). However, at the end of the
261 incubation, when the f_{OM} of the humified sediment was only 20% more than that of the raw
262 sediment without the SOM input, the K_d was still more than doubled. The change of
263 adsorption was not only influenced by the quantity, but also by the property. The curvature
264 index $1/n$ in the Freundlich model for BPA adsorption also decreased from 0.97 to 0.89,
265 showing a more curved adsorption isotherm after SOM decay. This change is consistent with
266 previous findings showing that the pattern of chemical adsorption by organic materials
267 becomes more curved after organic decomposition (Hur et al., 2011; Plaza et al., 2009).

268 The desorption experiment showed that the desorption-based partition coefficient for
269 BPA also decreased by 56% for the incubated sediment, which was still higher than the raw
270 sediment (Table 2). Moreover, desorption hysteresis was found for BPA desorption from the
271 sediment. Hysteresis is a result of partially irreversible adsorption, and the HI value has been
272 used to quantify the irreversibility of chemical adsorption (Wu and Sun, 2010). The BPA
273 desorption results indicated that HI increased continuously and significantly for the incubated
274 sediment. The HI change also correlated well with the transformation of SOM during
275 incubation, as chemical adsorption by condensed SOM is theoretically stronger, and chemical
276 desorption by more condensed SOM is harder than that by less condensed SOM (Gunasekara
277 and Xing, 2003).

278 **3.3 Adsorption and desorption of EE2**

279 Similar to BPA, the isotherm of EE2 adsorption by the incubated sediment also fits well
280 with the linear partition model ($R^2 \geq 0.95$) for the sediment samples after various incubation
281 periods (Fig. 4), whilst the curvature index $1/n$ in the Freundlich model is close to 1 (Table 2).

282 The fresh SOM into the sediment increased the adsorption affinity as well as the isotherm
283 linearity (Table 2, raw sediment and 0 day sediment). The fish food pellets with rich contents
284 of proteins and lipids apparently enhanced the adsorption capacity of the sediment and
285 changed the shape of its adsorption isotherm.

286 For the change of adsorption along with the incubation time, K_d initially decreased, but
287 recovered in the later phase. Within the first 2 months of sediment incubation, the K_d value
288 decreased by 43%, which correlated well with the rapid f_{OM} reduction in the sediment. K_d
289 then began to increase after about 2 months of sediment incubation and eventually reached 73%
290 of its initial value. In the later phase of sediment incubation, a large portion of the SOM
291 would have been transformed from simple hydrocarbons and fresh biomass to more
292 humic-like substances with more carboxylic and aromatic groups (Farnet et al., 2009). Such
293 SOM transformation is more favorable to the adsorption of EE2 molecules by the incubated
294 sediment, probably through π - π bonds and hydrogen bonds (Yamamoto et al., 2003).

295 As the desorption K_d values obtained were lower than the corresponding adsorption K_d
296 values, the desorption HI could not be derived for EE2. Consistent with the change in the
297 adsorption isotherm, the K_d value determined for the desorption of EE2 also decreased
298 initially before reversing direction and increasing (Table 2). The K_d decrease was most
299 significant in the first month, which correlated well with the rapid f_{OM} reduction observed.

300 **3.4 Adsorption of Phe**

301 A much greater amount of adsorption by the sediment was observed for Phe (Table 2).
302 Comparison between the raw sediment with SOM added sediment demonstrated that the
303 SOM addition greatly enhanced the sorption capacity to the sediment, as the K_d value
304 increased from 132.5 to 4430 kg/L. The I/n values for Phe were higher than 1 for some of the
305 aged sediment. This might be contributed to multilayer adsorption, as the sediment surface
306 would be modified by the Phe adsorption, leading to more and stronger adsorption. In

307 comparison to BPA and EE2, the partition coefficient of Phe showed a lower degree of
308 change during the sediment incubation. Its K_d value initially increased by 11% before
309 decreasing from 5612 on 15 day to 4686 L/Kg on 54 day (Table 2). The adsorption then
310 began to recover, eventually reaching to a level of around 5000 L/kg. It has been reported that
311 the sorption of Phe on SOM is mainly driven by hydrophobic effects (Wang et al., 2011). The
312 hydrophobic carbon content (the sum of alkyl and aromatic carbon content) was expected to
313 increase in the later phase of SOM decay in the incubated sediment (Hur et al., 2011), which
314 would lead to more and stronger nonspecific Phe bindings by the sediment for adsorption.

315 The strong degree of Phe adsorption by the sediment meant the surfactant SDBS had to
316 be used for the desorption tests. As a result, the partition coefficients of the desorption
317 isotherms were much lower than those of the adsorption isotherms and hence could not be
318 compared with the latter. Nonetheless, an increasing trend in desorption K_d became apparent
319 as the sediment incubation progressed, which also indicated stronger Phe adsorption by the
320 incubated sediment.

321 Data fitting with the Frunelich model showed the isotherm of Phe adsorption by the
322 incubated sediment became more non-linear in the later phase of sediment incubation (Table
323 2). The curvature index $1/n$ increased from 1.02 at the beginning of the incubation period to
324 more than 1.50 by the end. A value of $1/n > 1$ often indicates easier and stronger partitioning
325 at higher concentrations (Voice and Weber, 1983). It is apparent that the SOM was converted
326 to more condensed and humic-like materials with a strong binding affinity to Phe (Grathwol,
327 1990; Plaza et al., 2009).

328 **3.5 K_{OM} for BPA, EE2, and Phe**

329 SOM in sediment is believed to be the main adsorbent for chemical adsorption (e.g. Sun
330 et al., 2010; Wu and Sun, 2010; Xu et al., 2008). SOM normalized K_d was determined for the
331 model compounds (Fig. 5) using the K_d values and f_{OM} . The average $\text{Log}K_{OM}$ values were 2.2,

332 2.9, and 4.7 for BPA, EE2, and Phe, respectively. In other words, among the selected
333 contaminants, BPA was in all instances adsorbed the least and Phe was adsorbed the most by
334 the SOM after various periods of incubation. This is consistent with the common
335 understanding that the adsorption or partition of hydrophobic contaminants correlates
336 strongly with the hydrophobicity of the chemical molecules (Chiou et al., 1979; Voice and
337 Weber, 1983). In comparison to EE2 and Phe, BPA has a much lower K_{ow} and a much higher
338 S_w value (Table 1), which probably gives rise to its weak affinity with sediment organics and
339 hence its lowest level of adsorption by the sediment. Karickhoff et al. (1979) developed the
340 following relationship between the adsorption coefficient and the adsorbate hydrophobicity,

$$341 \quad \text{Log } K_{oc} = \text{Log } K_{ow} - 0.21. \quad (5)$$

342 Based on this correlation, the $\text{Log}K_{oc}$ values of the studied chemicals could be calculated as
343 2.0, 3.9, and 4.4 for BPA, EE2, and Phe, respectively. Comparison between the experimental
344 K_{OM} and the predicted values, a disagreement for EE2 can be found, as the K_{OM} determined
345 for EE2 was lower than expected. This result might have been affected by other factors,
346 besides the hydrophobic properties, such as the molecular size and structure of the chemicals
347 (Sun et al., 2010). For instance, the molecular size of EE2 is larger than that of BPA, which
348 would be an impediment for EE2 molecules accessing some adsorption sites. This could be
349 one of the more likely reasons for the difference in K_{OM} between EE2 and Phe being greater
350 than that predicted from the K_{ow} values alone.

351 The K_{OM} values were found to undergo various changes rather than staying constant
352 during the sediment incubation period. A general trend of increasing-delay-increasing could
353 be used to characterize the K_{OM} values for EE2 and Phe. Despite the great difference in values,
354 the K_{OM} for BPA, EE2, and Phe increased sharply within the first 15 days of incubation (Fig.
355 5). This correlates well with the period when the microbial activity increased greatly in the

356 sediment, as indicated by the rapid SOM degradation (Fig. 1) in the present work and
357 observed in our previous studies (Fei et al., 2011).

358 Afterwards, there was a slight decrease in K_{OM} for BPA and EE2, followed by a rather
359 stable pattern of values over a long period (d 33-75). During this period, SOM decomposition
360 became slower (Fig. 1), with biomass decay in the sediment (Fei et al., 2011). According to
361 the analysis of humic substances (Fig. 2), the humification process was in progress, though
362 not dramatically yet. The decrease of active biomass possibly caused the decrease of K_{OM} for
363 BPA and EE2. However, the inconspicuous transformation of SOM fractions might offset
364 this loss and keep the K_{OM} stable for a period.

365 Subsequently, biodegradable SOM was exhausted and biomass decay became more
366 important, when humic-like substances accumulated remarkably in the sediment (Fig. 2)..
367 The SOM was further converted into more condensed humic-like substances with more
368 aromatic, phenolic, carboxyl and other functional groups (Farnet et al., 2009) with higher
369 chemical adsorption capacities to hydrophobic chemicals (Gunasekara and Xing, 2003; Hur
370 et al., 2011). Owing to the SOM degradation and humification, K_{OM} increased by 111% and
371 38% for Phe and EE2, respectively (Fig. 5). Thus, SOM input and decomposition in the
372 sediment had a profound impact on its adsorption behavior and capacity.

373 Noticeably, K_{OM} of BPA did not increase at the end, but decreased by 42% (Fig. 5). The
374 different 'increasing' levels were found to be well consistent with the chemical
375 hydrophobicity, following the sequence of BPA<EE2<Phe. This result was similar to that
376 obtained by Sun et al. (2012), which reported that the adsorption of BPA, EE2, and Phe
377 decreased, insignificant changed, and increased, respectively. For the reason that Phe might
378 be much more dependent on the hydrophobic interactions than BPA (Sun et al., 2012), the
379 changes in the polarity and accumulation of aromatic structures of SOM would bring much
380 more significant effect on the increased hydrophobic adsorption to Phe. For relatively

381 hydrophilic molecules like BPA, however, the shifted SOM structure might not be able to
382 make positive impact. As for the differences among chemicals with varied chemical
383 properties, a conceptual model is presented in SI, which would help explain the possible
384 changing process of sediment adsorption in relation to SOM decomposition.

385 **4 Conclusions**

- 386 • Fresh SOM (fish food pellets) in marine sediment was decomposed during a 4-month
387 incubation. Extraction and analysis of humic-like substances suggest a humification-like
388 process during the sediment and SOM incubation.
- 389 • The adsorption behaviors of the 3 model micropollutants (BPA, EE2 and Phe) was
390 significantly influenced by the SOM decomposition. The K_d for BPA and EE2 decreased
391 by 70% and 28%, respectively, while for Phe increased by 11%.
- 392 • Generally, a 3-stage change for K_{OM} could be summarized. K_{OM} of the model chemicals
393 all increased at the beginning. After a period of delaying, it continued to increase for EE2
394 and Phe. For BPA, which was less hydrophobic, the K_{OM} decreased eventually.

395 **Acknowledgments**

396 This study was supported by grants AoE/P-04/2004 from the University Grants Council
397 (UGC) and ECF09/2011 from the Environment and Conservation Fund (ECF) of the Hong
398 Kong SAR Government. The technical assistances provided by Mr. Keith C.H. Wong and Mr.
399 Hamid Mashayekhi are highly appreciated.

400

401 **References**

402 Beaudoin, A., 2003. A comparison of two methods for estimating the organic content of
403 sediments. *J. Paleolimnol.* 29, 387-390.

404 Chiou, C.T., Peters, L.J. and Freed, V.H., 1979. Physical concept of soil-water equilibria for
405 non-ionic organic-compounds. *Science* 206, 831-832.

406 Colborn, T., Saal, F.S.V. and Soto, A.M., 1993. Development effects of endocrine-disrupting
407 chemicals in wildlife and humans. *Environ. Health Persp.* 101, 378-384.

408 Collins, T.J., 2008. Persuasive communication about matters of great urgency: Endocrine
409 disruption. *Environ. Sci. Technol.* 42, 7555-7558.

410 Cornelissen, G. and Gustafsson, O., 2004. Sorption of phenanthrene to environmental black
411 carbon in sediment with and without organic matter and native sorbates. *Environ. Sci.*
412 *Technol.* 38, 148-155.

413 Cornelissen, G., Gustafsson, O., Bucheli, T.D., Jonker, M.T.O., Koelmans, A.A. and Van
414 Noort, P.C.M., 2005. Extensive sorption of organic compounds to black carbon, coal, and
415 kerogen in sediments and soils: Mechanisms and consequences for distribution,
416 bioaccumulation, and biodegradation. *Environ. Sci. Technol.* 39, 6881-6895.

417 deBruyn, A.M.H. and Gobas, F.A.P.C., 2004. Modelling the diagenetic fate of persistent
418 organic pollutants in organically enriched sediments. *Ecol. Model.* 179, 405-416.

419 Droussi, Z., D'Orazio, V., Hafidi, M. and Ouattmane, A., 2009. Elemental and spectroscopic
420 characterization of humic-acid-like compounds during composting of olive mill
421 by-products. *J. Hazard. Mater.* 163, 1289-1297.

422 Farnet, A.M., Prudent, P., Ziarelli, F., Domeizel, M. and Gros, R., 2009. Solid-state (13)C
423 NMR to assess organic matter transformation in a subsurface wetland under cheese-dairy
424 farm effluents. *Biores. Technol.* 100, 4899-4902.

425 Fei, Y.H., Li, X.D. and Li, X.Y., 2011. Organic diagenesis in sediment and its impact on the
426 adsorption of bisphenol A and nonylphenol onto marine sediment. *Mar. Pollut. Bull.* 63,
427 578-582.

428 Fei, Y.H. and Li, X.Y., 2013. Adsorption of tetracyclines on marine sediment during organic
429 matter diagenesis. *Water Sci. Technol.* 67, 2616-2621.

430 Gao, J.P., Maguhn, J., Spitzauer, P. and Kettrup, A., 1998. Sorption of pesticides in the
431 sediment of the Teufelsweiher pond (Southern Germany)–I: Equilibrium assessments,
432 effect of organic carbon content and pH. *Water Res.* 32, 1662-1672.

433 Gobas, F.A.P.C. and MacLean, L.G., 2003. Sediment-water distribution of organic
434 contaminants in aquatic ecosystems: The role of organic carbon mineralization. *Environ.*
435 *Sci. Technol.* 37, 735-741.

436 Gong, J., Ran, Y., Chen, D.Y. and Yang, Y., 2011. Occurrence of endocrine-disrupting
437 chemicals in riverine sediments from the Pearl River Delta, China. *Mar. Pollut. Bull.* 63,
438 556-563.

439 Guo, X.Y., Wang, X.L., Zhou, X.Z., Ding, X., Fu, B., Tao, S. and Xing, B.S., 2013. Impact
440 of the simulated diagenesis on sorption of naphthalene and 1-naphthol by soil organic
441 matter and its precursors. *Environ. Sci. Technol.* 47, 12148-12155.

442 Gunasekara, A.S. and Xing, B.S., 2003. Sorption and desorption of naphthalene by soil
443 organic matter: Importance of aromatic and aliphatic components. *J. Environ. Qual.* 32,
444 240-246.

445 Hur, J., Lee, B.M. and Shin, H.S., 2011. Microbial degradation of dissolved organic matter
446 (DOM) and its influence on phenanthrene-DOM interactions. *Chemosphere* 85,
447 1360-1367.

448 Johnson, M.D., Huang, W. and Weber, W.J., 2001. A distributed reactivity model for
449 sorption by soils and sediments. 13. Simulated diagenesis of natural sediment organic
450 matter and its impact on sorption/desorption equilibria. *Environ. Sci. Technol.* 35,
451 1680-1687.

452 Karickhoff, S.W., Brown, D.S and Scott, T.A., 1979. Sorption of hydrophobic pollutants on
453 natural sediments. *Water Res.* 13, 241-248.

454 Mnif, W., Zidi, I., Hassine, A.I.H., Gomez, E., Bartegi, A., Roig, B. and Balaguer, P., 2012.
455 Monitoring endocrine disrupter compounds in the Tunisian hamdoun river using in vitro
456 bioassays. *Soil Sediment Contam.* 21, 815-830.

457 Plaza, C., Xing, B., Fernandez, J.M., Senesi, N. and Polo, A., 2009. Binding of polycyclic
458 aromatic hydrocarbons by humic acids formed during composting. *Environ. Pollut.* 157,
459 257-263.

460 Ran, Y., Sun, K., Ma, X.X., Wang, G.H., Grathwohl, P. and Zeng E.Y., 2007. Effect of
461 condensed organic matter on solvent extraction and aqueous leaching of polycyclic
462 aromatic hydrocarbons in soils and sediments. *Environ. Pollut.* 148, 529-538.

463 Sun, K., Gao, B., Zhang, Z.Y., Zhang, G.X., Liu, X.T., Zhao, Y. and Xing, B.S., 2010.
464 Sorption of endocrine disrupting chemicals by condensed organic matter in soils and
465 sediments. *Chemosphere* 80, 709-715.

466 Sun, K., Jin, J., Gao, B., Zhang, Z.Y., Wang, Z.Y., Pan, Z.Z., Xu, D.Y. and Zhao, Y., 2012.
467 Sorption of 17 α -ethinyl estradiol, bisphenol A and phenanthrene to different size fractions
468 of soil and sediment. *Chemosphere* 88, 577-583.

469 Van de Wiele, T., Vanhaecke, L., Boeckert, C., Peru, K., Headley, J., Verstraete, W. and
470 Siciliano, S., 2005. Human colon microbiota transform polycyclic aromatic hydrocarbons
471 to estrogenic metabolites. *Environmental Health Perspectives* 113, 6-10.

472 Voice, T.C. and Weber, W.J., 1983. Sorption of hydrophobic compounds by sediments, soils
473 and suspended-solids-1. Theory and background. *Water Res.* 17, 1433-1441.

474 Wang, H.S., Liang, P., Kang, Y., Shao D.D., Zheng, G.J., Wu, S.C., Wong, C.K.C. and Wong,
475 M.H., 2010. Enrichment of polycyclic aromatic hydrocarbons (PAHs) in mariculture
476 sediments of Hong Kong. *Environ. Pollut.* 158, 3298-3308.

477 Wang, P. and Keller, A.A., 2009. Partitioning of hydrophobic pesticides within a
478 soil-water-anionic surfactant system. *Water Res.* 43, 706-714.

479 Wang, X.L., Guo, X.Y., Yang, Y., Tao, S. and Xing, B.S., 2011. Sorption mechanisms of
480 phenanthrene, lindane, and atrazine with various humic acid fractions from a single soil
481 sample. *Environ. Sci. Technol.* 45, 2124-2130.

482 Weber, W.J., Huang, W.L. and LeBoeuf, E.J., 1999. Geosorbent organic matter and its
483 relationship to the binding and sequestration of organic contaminants. *Colloid. Surface. A*
484 151, 167-179.

485 Wu, W.L. and Sun, H.W., 2010. Sorption-desorption hysteresis of phenanthrene - Effect of
486 nanopores, solute concentration, and salinity. *Chemosphere* 81, 961-967.

487 Xing, B.S. and Pignatello, J.J., 1997. Dual-mode sorption of low-polarity compounds in
488 glassy poly(vinyl chloride) and soil organic matter. *Environ. Sci. Technol.* 31, 792-799.

489 Xing, B.S. and Pan, B., 2010. Competitive and complementary adsorption of bisphenol A and
490 17 alpha-ethinyl estradiol on carbon nanomaterials. *J. Agr. Food Chem.* 58, 8338-8343.

491 Xu, X.R., Wang, Y.X. and Li, X.Y., 2008. Sorption behavior of bisphenol A on marine
492 sediments. *J. Environ. Sci. Heal. A* 43, 239-246.

493 Xu, J., Yin, K., Lee, J.H.W., Liu, H., Ho, A.Y.T., Yuan, X. and Harrison, P.J., 2010.
494 Long-term and seasonal changes in nutrients, phytoplankton biomass, and dissolved
495 oxygen in Deep Bay, Hong Kong. *Estuar. Coast.* 33, 399-416.

496 Yamamoto, H., Liljestrand, H.M., Shimizu, Y. and Morita, M., 2003. Effects of
497 physical-chemical characteristics on the sorption of selected endocrine disruptors by
498 dissolved organic matter surrogates. *Environ. Sci. Technol.* 37, 2646-2657.

499 Yang, Y., Zhang, N., Xue, M. and Tao, S., 2010. Impact of soil organic matter on the
500 distribution of polycyclic aromatic hydrocarbons (PAHs) in soils. *Environ. Pollut.* 158,
501 2170-2174.

502 Zhao, Q., Weise, L., Li, P.J., Yang, K., Zhang, Y.Q., Dong, D.B., Li, P. and Li, X.J., 2010.
503 Ageing behavior of phenanthrene and pyrene in soils: A study using sodium
504 dodecylbenzenesulfonate extraction. *J. Hazard. Mater.* 183, 881-887.

Table 1 - Chemical properties of the selected micropollutants: BPA, EE2, and Phe (Sun et al., 2011).

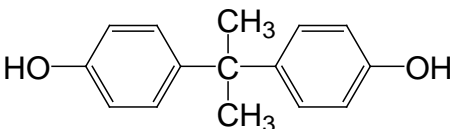
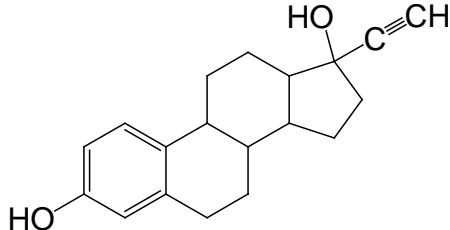
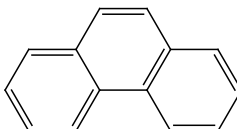
	BPA	EE2	Phe
Molecular structure			
Molecular diameter (Å)	4.3	6.0	5.6
Water solubility, S_w (mg/L)	380	7.6	1.12
Octanol-water distribution coefficient, $\text{Log}K_{ow}$	2.20	4.15	4.57

Table 2 - Summary of the adsorption and desorption isotherms of BPA, EE2, and Phe for the sediment after various periods of incubation.

Chemicals	Incubation time (d)	Adsorption					Desorption		
		Linear model		Freundlich model			Linear model		Hysteresis index (HI, %)
		K_d (L/kg)	R^2	Log K_F	$1/n$	R^2	K_d (L/kg)	R^2	
BPA	Raw sediment	4.15±0.15	0.99	1.07±0.022	0.71±0.021	1.00	6.71±0.53	0.97	61.69
	0	34.88±0.76	0.99	1.56±0.021	0.97±0.019	1.00	41.07±0.93	0.99	17.75
	15	26.69±0.86	0.98	1.49±0.043	0.94±0.042	0.99	33.17±1.75	0.97	24.28
	33	16.07±0.29	0.99	1.26±0.029	0.94±0.031	1.00	24.71±1.29	0.97	53.76
	54	12.93±0.34	0.99	1.25±0.024	0.89±0.024	1.00	19.20±0.45	0.99	48.49
	75	12.31±0.21	1.00	1.18±0.022	0.92±0.017	1.00	19.67±1.38	0.95	59.79
	96	13.54±0.31	0.99	1.22±0.031	0.92±0.032	1.00	22.41±1.47	0.96	65.51
	125	10.60±0.17	0.99	1.16±0.018	0.89±0.02	1.00	18.08±1.70	0.92	70.57
EE2	Raw sediment	25.27±0.98	0.97	1.48±0.009	0.77±0.022	0.99	9.83±0.95	0.89	-
	0	100.08±3.74	0.95	2.02±0.018	1.02±0.079	0.97	45.18±3.12	0.85	-
	15	89.94±2.67	0.97	1.95±0.020	1.12±0.072	0.98	45.49±1.69	0.96	-
	33	61.40±1.94	0.96	1.81±0.019	0.99±0.074	0.97	25.53±1.21	0.93	-
	54	57.49±1.39	0.98	1.75±0.012	1.07±0.049	0.99	22.28±1.99	0.76	-
	75	59.82±1.81	0.97	1.82±0.022	0.91±0.063	0.97	23.77±2.09	0.76	-
	96	63.02±1.53	0.98	1.82±0.019	1.00±0.055	0.98	27.30±1.73	0.87	-
	125	73.05±2.63	0.98	1.80±0.027	1.33±0.11	0.96	26.95±1.98	0.84	-
Phe	Raw sediment	132.5±3.3	0.98	1.98±0.038	1.13±0.049	0.99	6.47±0.74	0.92	-

0	4430±168	0.95	3.66±0.19	1.02±0.18	0.93	36.00±1.49	0.98	-
15	5612±66	1.00	3.84±0.039	1.08±0.029	1.00	-	-	-
33	4962±158	0.98	3.95±0.12	1.24±0.10	0.98	36.49±2.28	0.97	-
54	4686±178	0.99	4.17±0.056	1.47±0.057	1.00	-	-	-
75	4731±182	0.99	4.20±0.068	1.49±0.057	1.00	47.58±1.83	0.96	-
96	4988±312	0.98	4.95±0.27	2.16±0.25	0.97	-	-	-
125	4916±264	0.95	4.27±0.24	1.54±0.22	0.95	51.59±4.47	0.95	-

“-”: invalid or not determined.

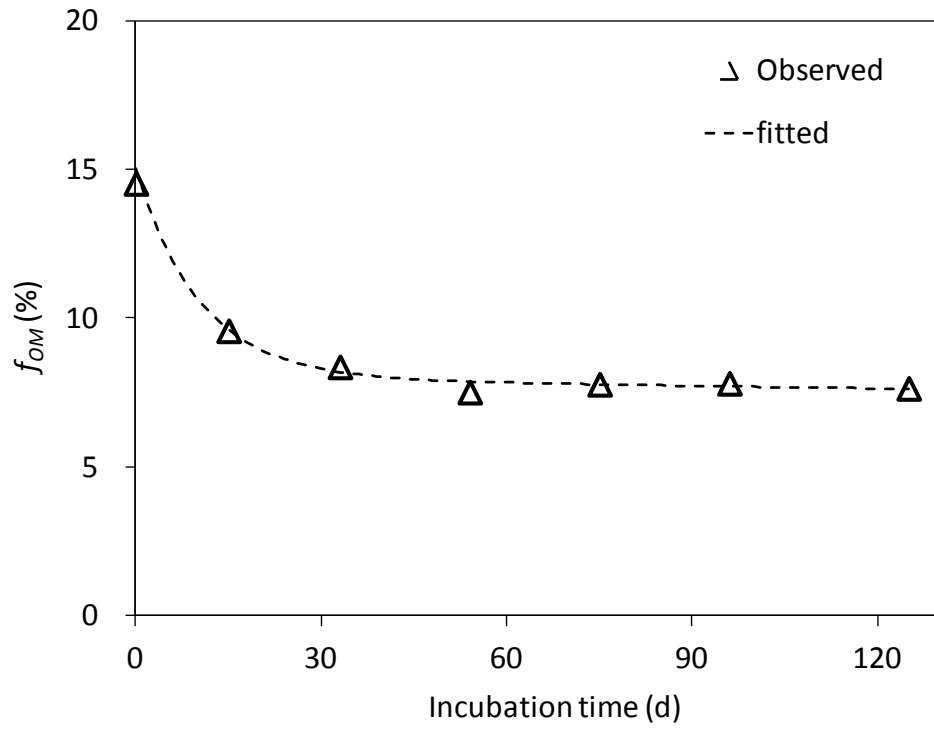


Fig. 1 - SOM reduction during the sediment incubation.

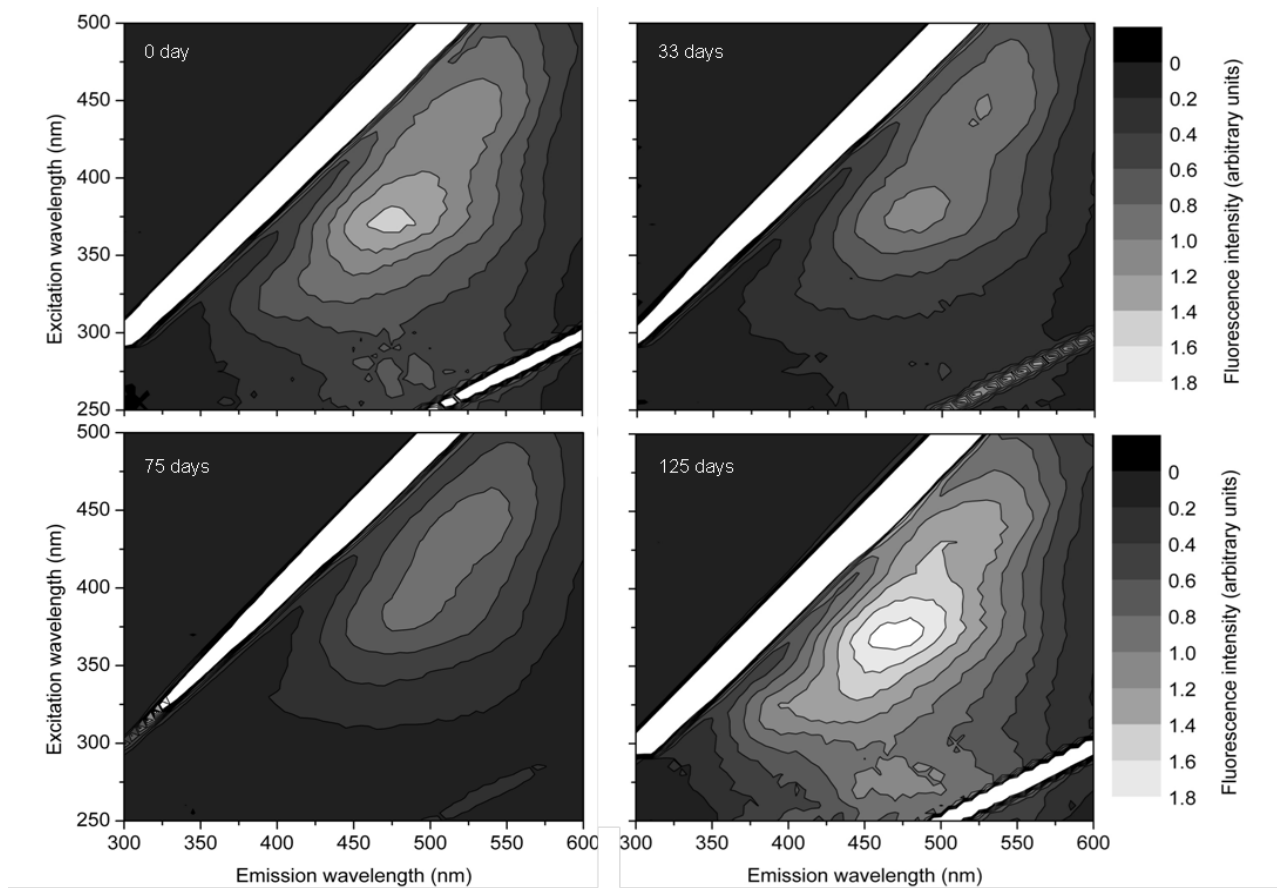


Fig. 2- FEEM of the humic substances extracted from the sediment samples after different incubation periods.

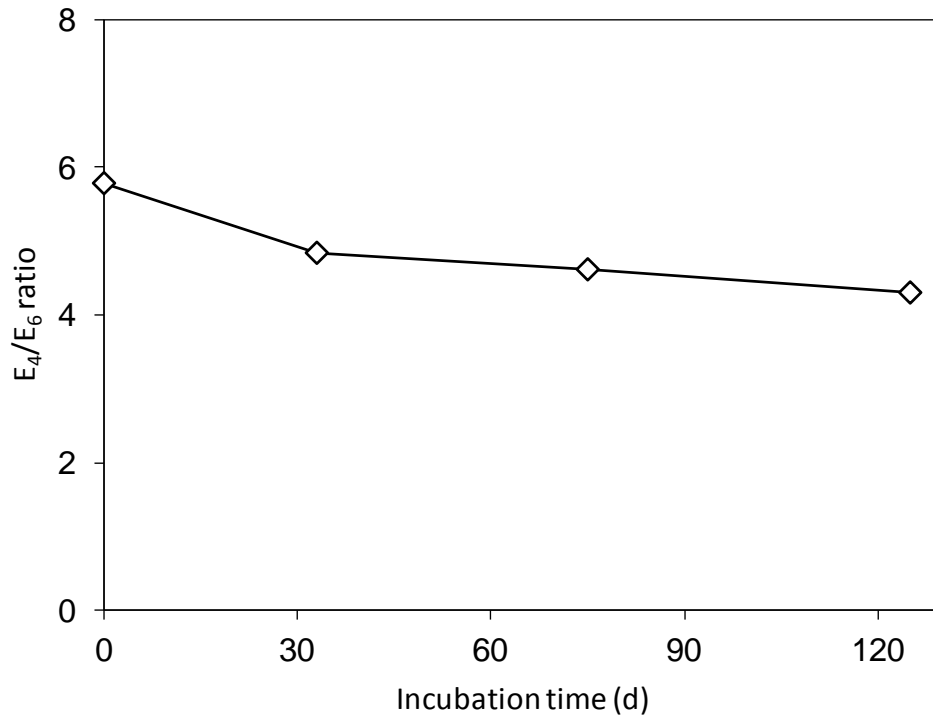


Fig. 3- E₄/E₆ ratio of the humic substances extracted from the sediment samples after different periods of sediment incubation.

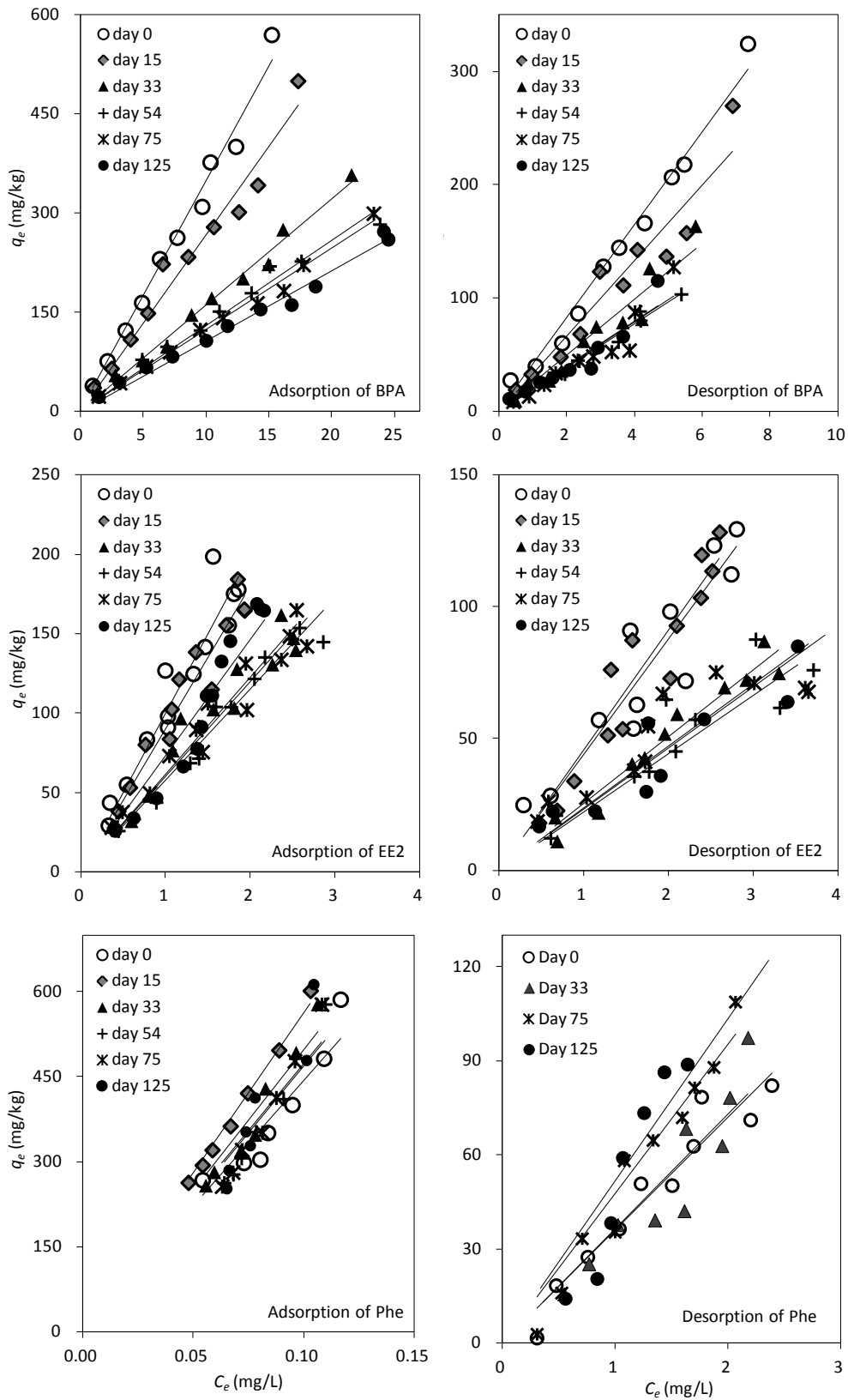


Fig. 4 - Isotherms of the adsorption and desorption of BPA, EE2, and Phe for the sediment samples after different periods of incubation.

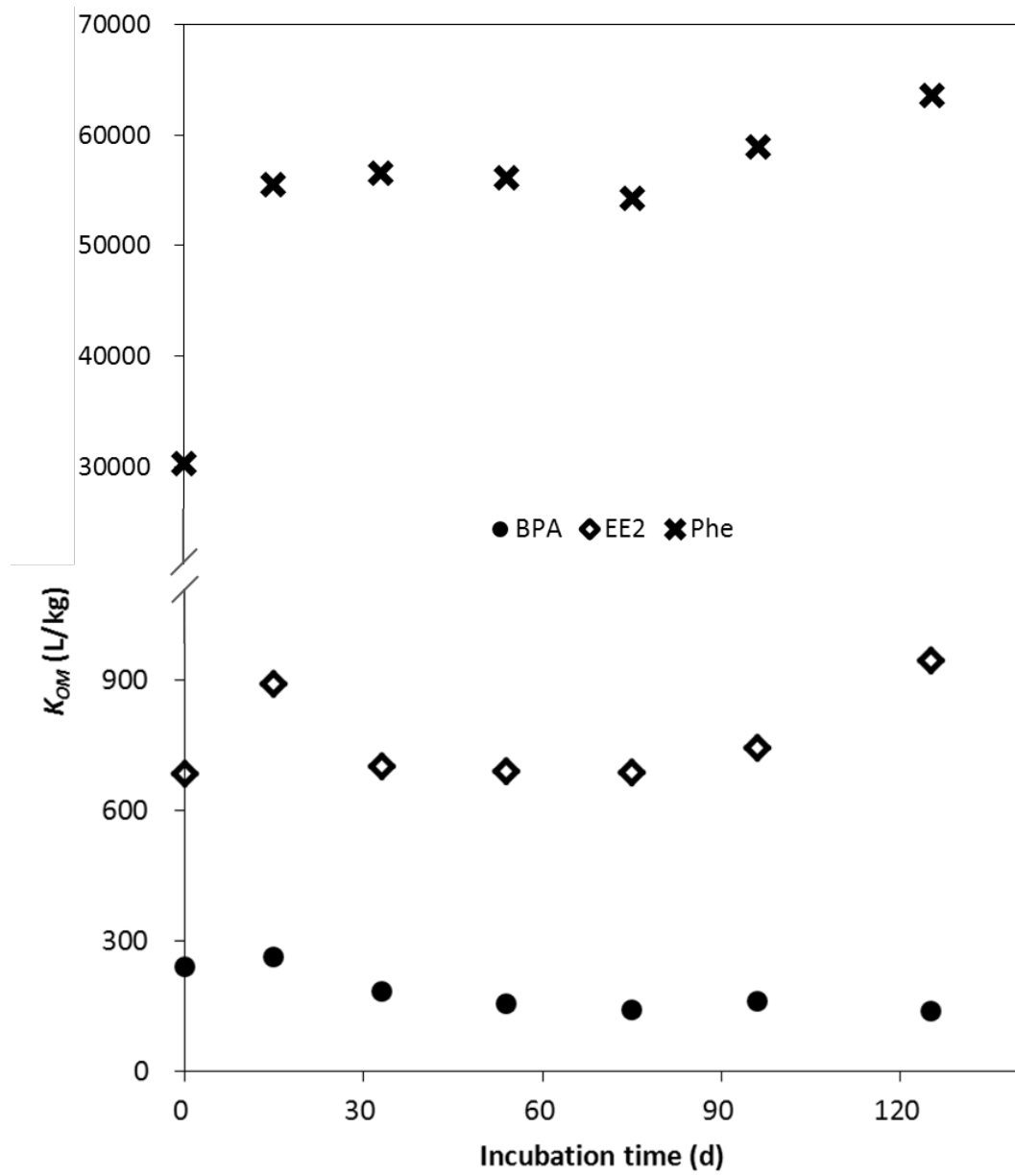


Fig. 5 - Changes in the K_{OM} values of BPA, EE2, and Phe with the sediment incubation time.

1 **Supplementary Material**

2

3 **Changes in the adsorption of bisphenol A, 17 α -ethinyl estradiol,**
4 **and phenanthrene on marine sediment in Hong Kong in relation**
5 **to the simulated sediment organic matter decomposition**

6

7 **Ying-heng Fei^{1, 2}, Baoshan Xing³, Xiao-yan Li^{1*}**

8 ¹ Department of Civil Engineering, The University of Hong Kong, Hong Kong, China

9 ² Water Science Research Center, Guangzhou Institute of Advanced Technology, Chinese
10 Academy of Sciences, Guangzhou, China

11 ³ Department of Plant, Soil and Insect Sciences, University of Massachusetts, Amherst,
12 MA, USA

13 (*Corresponding author: phone: 852-28592659; fax: 852-28595337; e-mail: xlia@hkucc.hku.hk)

14
15 The following supplementary materials are included:

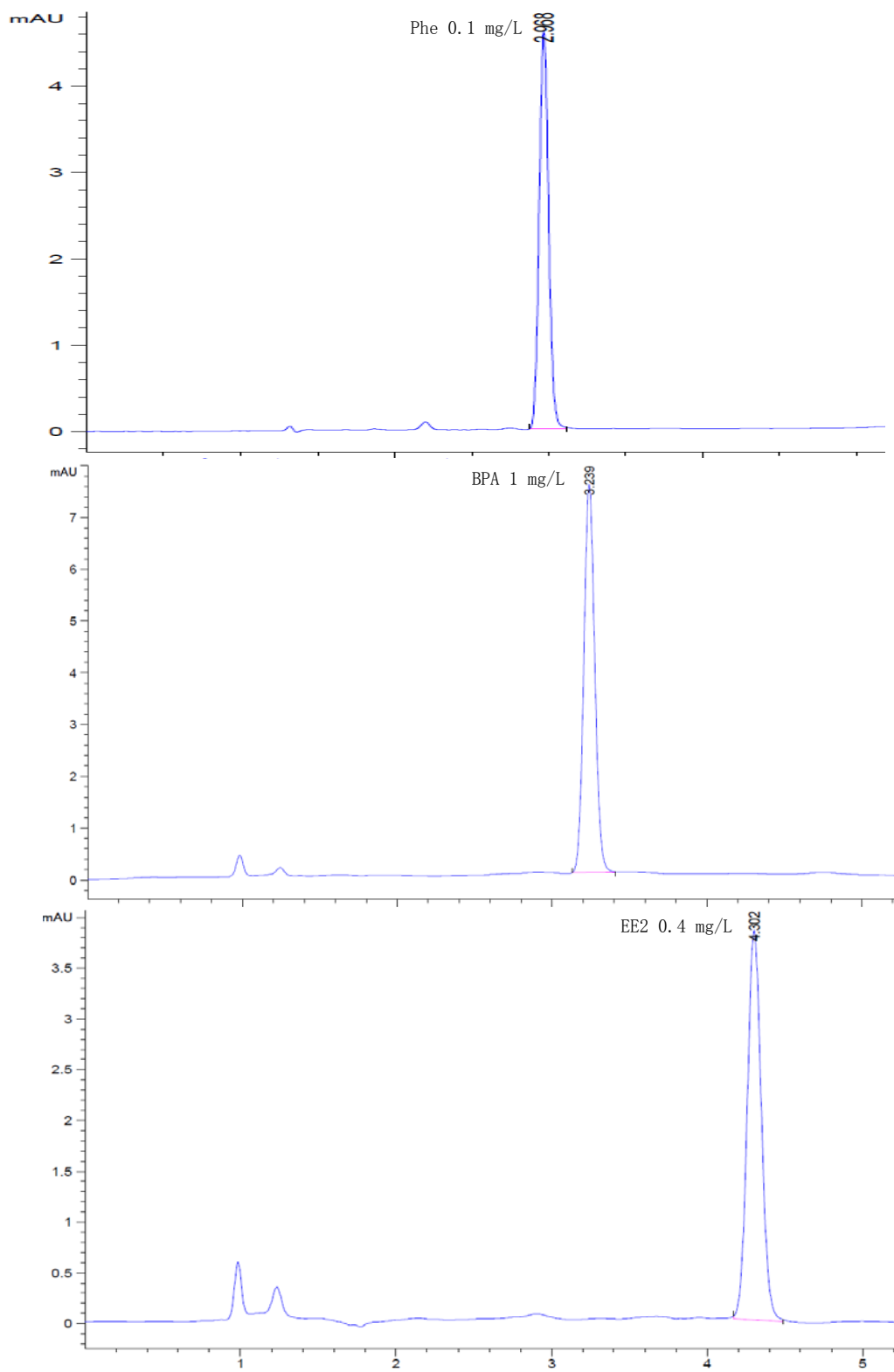
16 (1) HPLC chromatograph for BPA, EE2 and Phe detection.

17 (2) A conceptual model for SOM decay in sediment and its effect on adsorption capacity.

18

19 (1) HPLC chromatograph for BPA, EE2 and Phe detection

20



21

22

Fig. S1 - HPLC chromatograph for BPA, EE2 and Phe detection.

23

24 **(2) A conceptual model for SOM decay in sediment and its effect on adsorption**
25 **capacity**

26

27 The lab results reveal that fresh particulate matter deposited into sediment may not
28 behave as a stable entity for the transport of pollutants in the environment. SOM will undergo
29 various forms of degradation and diagenesis, and the aging process will alter the chemical
30 adsorption capacity of the sediment. However, in conventional chemical partition modeling
31 concerning SOM, a simple model of $K_d = f_{OM} K_{OM}$ is often used, in which all SOM
32 contents are grouped into the f_{OM} fraction with a single K_{OM} value. This study shows that such
33 a simplified approach cannot be employed to describe the dynamics of SOM degradation and
34 the resulting changes in adsorption capacity. It may be necessary to adopt a multi-fractional
35 approach to describe SOM transformation and its effect on sediment adsorption.

36 SOM input into sediment consists of multiple components in terms of biodegradability,
37 ranging from readily biodegradable organic matter to less degradable, refractory and
38 non-degradable organics (deBruyn and Gobas, 2004). Hence, the f_{OM} fraction can be written
39 as the sum of the finer individual SOM fractions, i.e.

40
$$f_{OM} = \sum_{i=1}^n f_{OM_i} \quad (S1)$$

41 where i signifies the i^{th} SOM fraction. The fraction f_{OM1} represents the most readily
42 biodegradable organic fraction, and as the i value increases, the SOM fraction becomes less
43 degradable.

44 In this experimental study, initial f_{OM} in the sediment was around 15%, including 5% of
45 raw organic in the Harbour sediment and 10% of fish food (SOM) added into the sediment.
46 Most of the raw SOM in the natural sediment could be considered refractory, while feeds in
47 the fish farms are usually believed to be predominated by labile organic matters (deBruyn and

48 Gobas, 2004). For the loaded fish food pellets that contains about 70% of proteins and lipids,
 49 and 30% of fibers and other carbohydrates, based on the product information, the fast- and
 50 slow-decomposing fractions with a ratio of 7:3 might be assumed (Jamu and Piedrahita, 2002;
 51 Arndt et al., 2013). Hence, the initial f_{OM} could be approximated into 3 components with a
 52 ratio of 7:3:5.

53 Assuming first-order kinetics for the degradation of different organic components in
 54 sediment, the fraction-based SOM reduction dynamics may be described by the following
 55 simplified form:

$$56 \quad f_{OM}^t = \sum_{i=1}^n f_{OM_i}^0 e^{-k_i t} \quad (S2)$$

57 where f_{OM}^t is the overall SOM content after period t , $f_{OM_i}^0$ stands for the i^{th} fraction of fresh
 58 SOM on day 0, and k_i is the rate constant of organic degradation for the i^{th} SOM fraction.
 59 Using the best fit for the SOM reduction results reported in Fig. S1 as an example, the
 60 following expression can be obtained for SOM degradation during sediment incubation:

$$61 \quad f_{OM}^t = 0.07e^{-0.096t} + 0.03e^{-0.0011t} + 0.05e^{-0t} \quad (S3)$$

62 This fitting result is comparable to organic decomposition rates observed by others. For
 63 instance, it has been reported that rapid and slow organic decay occur in the order of several
 64 per cents and tenths of a per cent per day in marine sediment, respectively, while recalcitrant
 65 organic substances in sediment can decay at the rate of 0.1% per year or lower (deBruyn and
 66 Gobas, 2004).

67 In relation to the SOM fractions, there should be a K_{OM} value for the adsorption of a
 68 given chemical pollutant by a particular f_{OM} fraction. Thus, the SOM-based partition
 69 coefficient may be written as

$$70 \quad K_d = \sum_{i=1}^n f_{OM_i} K_{OM_i} \quad (S4)$$

71 Furthermore, the overall K_{OM} value, or K_d/f_{OM} , can be calculated by

$$72 \quad K_{OM} = \sum_{i=1}^n \frac{f_{OM_i}}{f_{OM}} K_{OM_i} \quad (S5)$$

73 For each fraction, the fractional coefficient, K_{OM_i} , is a constant, as for that unchanged
74 chemical composition and structure is assumed for each subdivided fraction. Hence, the
75 change of SOM during organic composition was achieved by the alteration among different
76 fractions, instead of the chemical transformation inside each fraction. When SOM undergoes
77 humification, many SOM fractions, particularly the readily biodegradable fractions, i.e. f_{OM1} ,
78 f_{OM2} or f_{OM3} ..., will reduce over time. Thus, there could be a shift in the f_{OM_i} profile during the
79 sediment aging process. The f_{OM_i} for lower i SOM fractions will decrease significantly, and
80 the f_{OM_i} for the higher i fractions will hardly decrease and may even increase. As a result, the
81 f_{OM_i}/f_{OM} ratio will decrease greatly for lower i fractions and will increase considerably for
82 higher i fractions. In the present study, after 120 d of incubation the fractional ratio of f_{OM}
83 shifted to 0:2.5:5. As we can find out that, not only the SOM content decreased from 15% to
84 7.6%, and also the SOM fraction distribution was altered from f_{OM1} dominated to f_{OM3}
85 dominated.

86 The change in the f_{OM_i} profile during sediment aging will affect the chemical adsorption
87 capacity of the sediment. In comparison to more hydrophilic and biodegradable SOM, more
88 condensed humic-like SOM bring about more and stronger adsorption (Sun et al., 2010;
89 Weber et al., 1999). Thus, for hydrophobic micropollutants typically found in sediment, K_{OM_i}
90 values for lower i SOM fractions are generally lower than those for higher i fractions. If the
91 difference is only marginal for a particular chemical, i.e. $K_{OM_i} \approx K_{OM_j}$ ($i < j$), Eq. S5 suggests
92 that the change in the f_{OM_i} profile resulted from the SOM degradation will cause little change
93 in the overall K_{OM} value of the sediment. This is likely to have been the case for hydrophilic
94 chemicals, i.e. BPA observed in this study. However, SOM decay and reduction would still

95 lead to a continuous decrease in the K_d value of BPA in the sediment. If the difference is
96 significant, i.e. $K_{OMi} < K_{OMj}$ ($i < j$), the change in the f_{OMi} profile will result in a general
97 increase in the overall K_{OM} value, which is likely to have been the case for EE2 and Phe
98 observed here. If the difference is rather great, i.e. $K_{OMi} \ll K_{OMj}$ ($i < j$), the change in the f_{OMi}
99 profile would lead to a greater increase in K_{OM} . Moreover, the overall K_d value may not
100 decrease but increase with the SOM decay and f_{OM} reduction, as displayed by both Phe and
101 EE2 in the later phase of sediment incubation.

102 The model proposed here is basically a conceptual description for the analysis of
103 experimental observations on the change in chemical adsorption by sediment in relation to
104 SOM degradation. The great complexity of sediment and the dynamic changes in SOM
105 components mean determining f_{OMi} fractions and corresponding K_{OMi} values is extremely
106 difficult, if not impossible. To quantitatively validate it to a mathematical model, the SOM
107 fractionation as well as the determination of the assigned fractional K_{OM} need to be further
108 discussed, and the dynamic change of each fraction need to be carefully monitored. This
109 would be a follow-up study in the future. Nonetheless, the model and its underlying
110 mechanism provide a sound basis for predicting the impact of organic deposition and SOM
111 decomposition on the adsorption of environmental pollutants in marine sediment.

112

113 **References:**

- 114 Arndt, S., Jorgensen, B.B., LaRowa, D.E., Middelburg, J.J., Pancost, R.D. and Regnier, P.,
115 2013. Quantifying the degradation of organic matter in marine sediments: A review and
116 synthesis. *Earth-Sci. Rev.* 123, 53-86.
- 117 deBruyn, A.M.H. and Gobas, F.A.P.C., 2004. Modelling the diagenetic fate of persistent
118 organic pollutants in organically enriched sediments. *Ecol. Model.* 179, 405-416.

119 Jamu, D.M. and Piedrahita, R.H., 2002. An organic matter and nitrogen dynamics model for
120 the ecological analysis of integrated aquaculture/agriculture system: I. model
121 development and calibration. *Environ. Modell. Softw.* 17, 571-582.

122 Sun, K., Gao, B., Zhang, Z.Y., Zhang, G.X., Liu, X.T. Zhao, Y. and Xing, B.S., 2010.
123 Sorption of endocrine disrupting chemicals by condensed organic matter in soils and
124 sediments. *Chemosphere* 80, 709-715.

125 Weber, W.J., Huang, W.L. and LeBoeuf, E.J., 1999. Geosorbent organic matter and its
126 relationship to the binding and sequestration of organic contaminants. *Colloid Surface A*
127 151, 167-179.

128